Integrated polarizers based on tapered highly birefringent photonic crystal fibers

Priscila Romagnoli,[1,*] Claudecir R. Biazoli,[2] Marcos A. R. Franco,[3] Cristiano M. B. Cordeiro[2] and Christiano J. S. de Matos[1]

[1]*Graphene and Nano-Materials Research Center (MackGraphe), Mackenzie Presbyterian University, São Paulo, SP, Brazil*

[2]*Instituto de Física "Gleb Wataghin", Universidade Estadual de Campinas - UNICAMP, Campinas, SP, Brazil*

[3]*Computacional Electromagnetic Laboratory, Institute of Advanced Studies - IEAv,São José dos Campos, SP, Brazil*

[*]*priscilaromagnoli@yahoo.com.br*

Abstract: This paper proposes and demonstrates the creation of sections with a high polarization dependent loss (PDL) in a commercial highly birefringent (polarization maintaining) photonic crystal fiber (PCF), via tapering with pressure applied to the holes. The tapers had a 1-cm-long uniform section with a 66% scale reduction, in which the original microstructure aspect ratio was kept by the pressure application. The resulting waveguides show polarizing action across the entire tested wavelength range, 1510-1600 nm, with a peak PDL of 35.3 dB/cm (c.f. ~1 dB/cm for a typical commercial polarizing fiber). The resulting structure, as well as its production, is extremely simple, and enable a small section with a high PDL to be obtained in a polarization maintaining PCF, meaning that the polarization axes in the polarizing and polarization maintaining sections are automatically aligned.

OCIS codes: (060.5295) Photonic crystal fibers; (130.5440) Polarization-selective devices; (260.1440) Birefringence.

References and links

1. A. R. Chraplyvy, "High-capacity lightwave transmission experiments," Bell Labs Tech. J. **4**(1), 230–245 (1999).
2. W. J. Bock, J. Chen, T. Eftimov, and W. Urbanczyk, "A photonic crystal fiber sensor for pressure measurements," IEEE Trans. Instrum. Meas. **55**(4), 1119–1123 (2006).
3. R. A. Bergh, H. C. Lefevre, and H. J. Shaw, "An overview of fiber-optic gyroscopes," J. Lightwave Technol. **2**(2), 91–107 (1984).
4. W. Jacobsen, J. Mayfield, P. Fournier, D. Bolte, H. Elmaola, C. H. Wang, G. Drenzek, and A. Soufiane, "Single-polarization fiber," Verrillon Inc., US Patent 8,369,672 B2, (2013).
5. D. A. Nolan, G. E. Berkey, M. J. Li, X. Chen, W. A. Wood, and L. A. Zenteno, "Single-polarization fiber with a high extinction ratio," Opt. Lett. **29**(16), 1855–1857 (2004).
6. P. Russell, "Photonic crystal fibers," J. Lightwave Technol. **24**(12), 4729–4749 (2006).
7. K. Saitoh and M. Koshiba, "Single-polarization single-mode photonic crystal fibers," IEEE Photon. Technol. Lett. **15**(10), 1384–1386 (2003).
8. J. Ju, W. Jin, and M. S. Demokan, "Design of single-polarization single-mode photonic crystal fiber at 1.30 and 1.55 μm," J. Lightwave Technol. **24**(2), 825–830 (2006).
9. F. Zhang, M. Zhang, X. Liu, and P. Ye, "Design of wideband single-polarization single-mode photonic crystal fiber," J. Lightwave Technol. **25**(5), 1184–1189 (2007).
10. M. Y. Chen, B. Sun, and Y. K. Zhang, "Broadband single-polarization operation in square-lattice photonic crystal fibers," J. Lightwave Technol. **28**(10), 1443–1446 (2010).
11. V. A. Serrão and M. A. R. Franco, "A new approach to obtain single-polarization hollow-core photonic bandgap fiber," Proc. SPIE 8794, Fifth European Workshop on Optical Fibre Sensors, 879428 (2013).
12. H. Kubota, S. Kawanishi, S. Koyanagi, M. Tanaka, and S. Yamaguchi, "Absolutely single polarization photonic crystal fiber," IEEE Photon. Technol. Lett. **16**(1), 182–184 (2004).
13. G. Statkiewicz-Barabach, J. Olszewski, M. Napiorkowski, G. Golojuch, T. Martynkien, K. Tarnowski, W. Urbanczyk, J. Wojcik, P. Mergo, M. Makara, T. Nasilowski, F. Berghmans, and H. Thienpont, "Polarizing photonic crystal fiber with lowindex inclusion in the core," J. Opt. **12**(7), 075402 (2010).
14. X. Zheng, Y. Liu, Z. Wang, T. Han, and B. Tai, "Tunable single-polarization single mode photonic crystal fiber based on liquid infiltrating," IEEE Photon.Technol. Lett. **23**, 709–711 (2011).

#213127 - $15.00 USD Received 30 May 2014; revised 3 Jul 2014; accepted 7 Jul 2014; published 14 Jul 2014

15. A. V. Y. Espinel, M. A R. Franco, and C. M. B. Cordeiro, "Tunable single-polarization single-mode microstructure polymer optical fiber," J. Lightwave Technol. **29**(16), 2372–2378 (2011).
16. W. Qian, C. L. Zhao, Y. Wang, C. C. Chan, S. Liu, and W. Jin, "Partially liquid-filled hollow-core photonic crystal fiber polarizer," Opt. Lett. **36**(16), 3296–3298 (2011).
17. A. C. Sodré, Jr., A. R. Nascimento, Jr., M. A. R. Franco, I. Oliveira, V. A. Serrão, and H. L. Fragnito, "Numerical and experimental analysis of polarization properties from hybrid PCFs across different photonic bandgaps," Opt. Fiber Technol. **18**(6), 462–469 (2012).
18. P. Romagnoli, C. R. Biazoli, M. A. R. Franco, C. M. B. Cordeiro, and C. J. S. de Matos, "Generation of polarizing sections in highly birefringent photonic crystal fibers via post-processing," in CLEO:2013, (Optical Society of America, 2013), paper JTu4A.12.
19. T. A. Birks and Y. W. Li, "The shape of fiber tapers," J. Lightwave Technol. **10**(4), 432–438 (1992).
20. J. Ju, W. Jin, and Y. Yang, "Introduction of birefringence into photonic crystal fibers," Proc. SPIE 7753, 21st International Conference on Optical Fiber Sensors, 77536J (2011).
21. I. H. Malitson, "Interspecimen comparison of the refractive index of fused silica," J. Opt. Soc. Am. **55**(10), 1205–1209 (1965).
22. R. M. Gerosa, D. H. Spadoti, L. S. Menezes, and C. J. S. de Matos, "In-fiber modal Mach-Zehnder interferometer based on the locally post-processed core of a photonic crystal fiber," Opt. Express **19**(4), 3124–3129 (2011).

1. Introduction

Optical fiber devices for polarization management are essential components in fields such as optical telecommunications, in systems involving polarization multiplexing [1]; sensing, in schemes that use polarimetric and interferometric measurements to probe environmental parameters [2]; and inertial navigation, for the development of fiber gyroscopes [3]. In most cases, it is essential to obtain a single linear polarization, with sufficient suppression of the orthogonal polarization component. A means of obtaining such a condition in an all-fiber format is with fibers with a high polarization dependent loss (PDL), known as polarizing fibers. Usually, these fibers are comprised of an elliptical core, resulting in a high birefringence, with different confinement losses for each polarization mode; suppression of the lossier polarization is achieved along propagation. Commercial polarizing fibers typically present a PDL of 0.04~2.16dB/cm, centered at 1550 nm [4,5]. This means that, e.g., at least ~10 cm of fiber are required to obtain a PDL in excess of 20 dB. Also, for the generated polarization state to be kept along the fiber link, the polarizing fiber needs to be spliced to polarization maintaining fibers, and the polarization axes must be perfectly aligned.

Photonic crystal fibers (PCFs) [6] have been numerically proposed as polarizing fibers [7–10], which can be accomplished through careful design of the microstructure's pitch and hole diameters. In one design [7], the microstructure allowed for guidance in a single polarization, therefore theoretically achieving infinite PDL values. The proposed fiber included a photonic crystal cladding with a pitch to operating wavelength ratio, Λ/λ, of 1.42 and a hole diameter to pitch ratio, d/Λ, of 0.5. This relatively low d/Λ value induces a high cladding effective index, which approaches, and eventually coincides with, the fundamental core mode index as the wavelength increases. The design also included two lines of two or four holes with a larger diameter (hole diameter to pitch ratio, d'/Λ, of 0.95) in either side of the core, which induced a modal birefringence as high as $\sim 3 \times 10^{-3}$. The resulting break of degeneracy for the fundamental mode is then high enough to make the cladding and fundamental mode indices to match at significantly different wavelengths for the slow and fast polarization axes, thus generating the desired polarizing action over a 120 nm bandwidth. It is noted that the mentioned PCF design has not been experimentally demonstrated, possibly due to the relatively complex control over the three design parameter during the fiber drawing process.

Other methods for obtaining polarizing PCFs have also been studied [11–14]. Espinel *et al.* [15] numerically showed a microstructured polymer fiber for which the application of hydrostatic pressure induced birefringence and polarizing action. The obtained PDL was of the order of 0.38 dB/cm. Quian *et al.* [16] experimentally showed a polarizing PCF through partial filling of its microstructure with ethanol. The partial filling weakened modal confinement for one polarization, while the orthogonal polarization propagated with relatively

#213127 - $15.00 USD Received 30 May 2014; revised 3 Jul 2014; accepted 7 Jul 2014; published 14 Jul 2014

low loss. The reported PDL was approximately 30 dB/cm in the 1480-1600 nm range. Sodré Jr. *et al.* [17] experimentally demonstrated a hybrid PCF in which residual stress induced a PDL of the order of 0.2-0.5 dB/cm in different bandgaps. However, the proposed fibers mentioned here rely on structures that are difficult to fabricate or to achieve via post-processing techniques.

Here, we demonstrate the creation of a high PDL fiber section through post-processing of a commercial highly birefringent (polarization maintaining) PCF. The utilized post-processing technique is fiber tapering with the application of differential pressure to the microstructure holes, so that the cross-sectional aspect ratio is kept. Thereby, the initial birefringence increased as well as the confinement loss for one of the polarizations, resulting in a local polarizing action. The tapered section was 1 cm long and resulted in a PDL in excess of 10 dB/cm in the entire 1510-1600 nm tested range. The maximum measured PDL was as high as 35.3 dB/cm. Both the post-processing method and the resulting structure are simple to be obtained and enable flexibility and all-fiber integration in systems with high polarization constraints. A preliminary and briefer description of this work has been previously reported [18].

2. Design of high PDL sections

The aim of the present work is to obtain a fiber structure similar to that proposed by Saitoh *et al.* [7], but via post-processing of a commercially available highly birefringent PCF (PM-1550-01, by NKT Photonics), the cross section of which is shown in Fig. 1(a). This PCF has an array of holes with $d/\Lambda = 0.5$ (and $d = 2.2$ μm) and two larger holes positioned on opposite sides of the core (with $d'/\Lambda = 1.02$ and $d' = 4.5$μm). It is noted that both diameter-to-pitch ratios are rather similar to those of the fiber in [7]. However, as the Λ/λ ratio is twice as large (2.84 for an operating wavelength of 1550 nm), the resulting birefringence is almost an order of magnitude smaller (5.35×10^{-4}, determined by numerical simulation) and the cladding effective index is significantly lower than the fundamental mode indices, thus leading to negligible confinement losses for both polarizations. Comparison between these two fibers further suggests that a scale reduction in a section of the commercial PCF would result in similar propagation conditions to the fiber proposed in [7]. Fiber tapering [19] was then chosen as the post-processing technique to increase the initial birefringence of the commercial PCF [20], as well as to provide polarization dependent confinement loss.

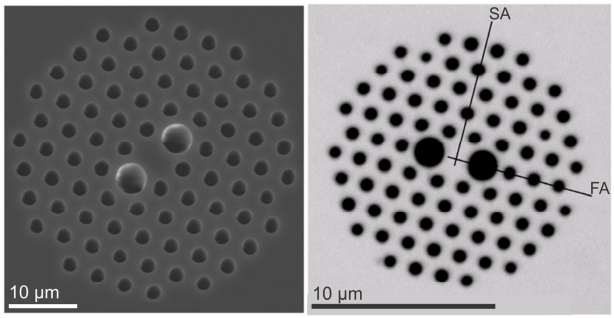

Fig. 1. Scanning electron micrographs of the commercially-available polarization maintaining PCF used in the experiments before (a) and after (b) tapering.

In order to check on this possibility, the commercial PCF was simulated using a commercial software based on the vectorial finite element method (COMSOL®). Perfectly matched layers (PML) were used for computational domain truncation and the silica refractive index was calculated by the Sellmeier equation [21]. Firstly, the PDL was numerically determined as a function of the amount of scale reduction, as shown in Fig. 2(a).

#213127 - $15.00 USD Received 30 May 2014; revised 3 Jul 2014; accepted 7 Jul 2014; published 14 Jul 2014

It can be noted that the PDL is maximized for a 70% of scale reduction. However, in this case the confinement loss for the lower loss polarization (slow axis mode) was as high as ~80.5 dB/cm. In contrast, a 66% of scale reduction presented a confinement loss of ~5.4 dB/cm and a PDL of 94.63 dB/cm, and therefore was chosen as the scale reduction target. The corresponding Λ/λ ratio at 1550 nm was 0.97. The resulting, tapered, structure was then simulated for a range of wavelengths from 1510 to 1590 nm. A constant birefringence of ~4.67×10^{-3} was obtained throughout this spectral region, which is one order in magnitude larger than the initial birefringence and is similar to that of the fiber proposed in [7].

As detailed in section 3, a section of the PCF was experimentally tapered to match the optimum 66% scale reduction, and an electron microscopy image of its cross section is shown in Fig. 1(b). To account for structural distortions during tapering, the resulting structure was then simulated. The confinement loss, at 1560 nm, at polarizations along the fiber's principal axes, fast axis (FA) and slow axis (SA), in Fig. 1(b), was calculated through the numerically obtained imaginary parts of the refractive indices. Figure 2(b) shows the light intensity distribution on the cross section of the fiber for both of fundamental mode polarizations. It can be seen that the slow-axis polarization is better confined in the core than the fast-axis polarization. Figure 2(c) shows the confinement loss for both polarizations, indicating that, indeed, the fast-axis mode is considerably lossier. For both polarizations, the loss increases with wavelength, as expected, with the loss of the fast-axis mode increasing faster and resulting in a PDL that increases with wavelength.

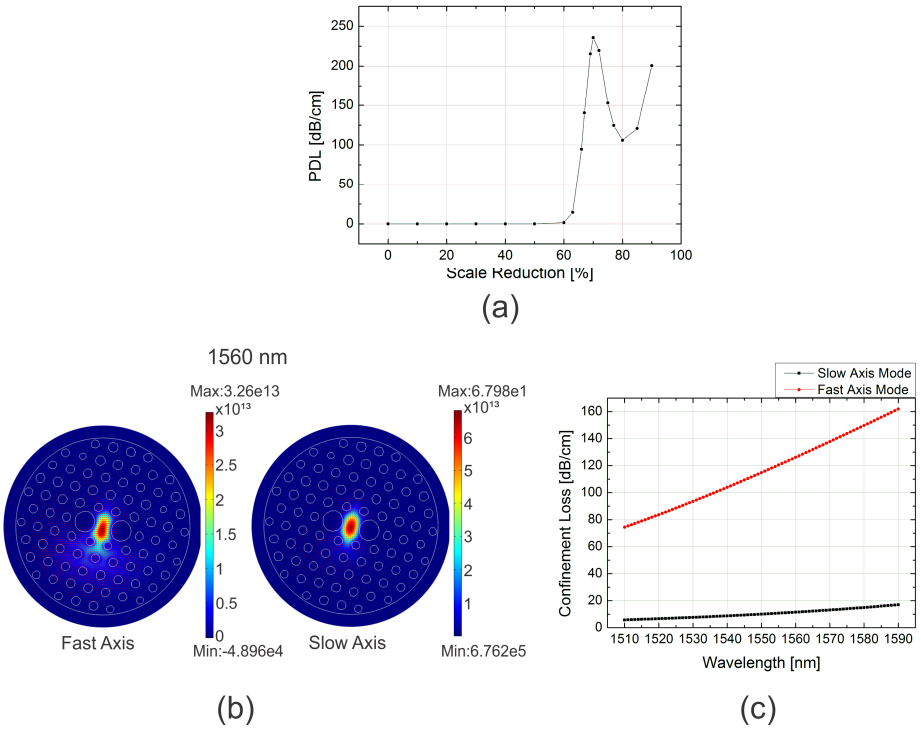

Fig. 2. (a) Simulated PDL as a function of the scale reduction factor. (b) Simulated light intensity distribution on the cross section of the tapered PCF. (c) Simulated confinement loss as a function of wavelength.

3. Production of the polarizing tapers

The setup of the tapering rig used to create the high PDL sections in the PCF can be seen in Fig. 3(a). It consists of a temperature-controlled isobutene and oxygen flame, which heats the section of the fiber to be tapered while DC motors pull it. To ensure that the holes do not

#213127 - $15.00 USD Received 30 May 2014; revised 3 Jul 2014; accepted 7 Jul 2014; published 14 Jul 2014

collapse and to keep their original relative dimensions (and, therefore, to keep d/Λ and d'/Λ constant), the smaller and larger holes in the microstructure are submitted to different nitrogen (N_2) pressures. For such a differential pressure distribution to be obtained, one tip of the PCF had the two larger holes blocked with a polymeric adhesive, which was deployed to the fiber facet with the use of a micropipette [22]; at the other fiber facet the small holes were collapsed by heating, while the larger holes were left opened. Thereby, by applying different pressures to the opposite fiber tips, the larger and smaller holes are independently pressurized. Several pairs of pressures were tested to keep the fiber's aspect ratio, with the best results obtained with 6 bars and 3 bars in the smaller and larger holes, respectively. The corresponding electron microscopy image can be seen in Fig. 1(b), which was obtained by cleaving one post-processed fiber at the tapered region. The tapered section has a 66% scale reduction, with d/Λ and d'/Λ ratios of 0.45 and 1.00, respectively, and a Λ/λ ratio of 1.05. All of these ratios are in very good agreement with the numerically optimized ratios for optimized PDL. A good reproducibility of the taper cross section was achieved when the same pressure values were used. Among different samples, the variation of the fiber's final parameters were measured to be ± 2% for the outer cladding diameter; ± 6% for Λ; ± 4% for d'; and ± 5% for d. The taper diameter as a function of fiber position for one sample was measured with an optical microscope and is shown in Fig. 3(b). The waist is 1.0 cm long, with transition regions of ~1.25 cm in length.

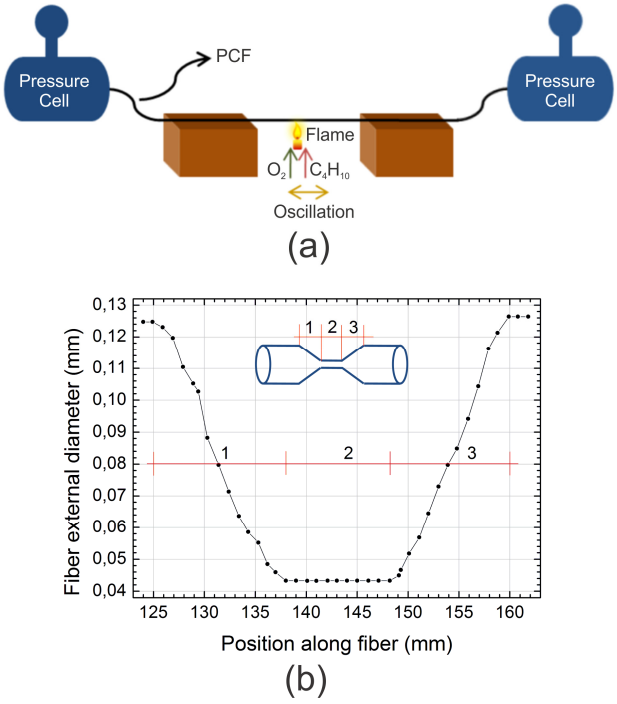

Fig. 3. (a) Tapering rig setup with differential pressure. (b) Tapered section profile: sections 1 and 3 are the transition regions, while section 2 is the down-tapered region with a constant diameter.

4. Optical characterization

The resulting tapered PCF structure was optically characterized in the 1510-1590 nm wavelength range. The characterization setup can be seen in Fig. 4 and consists of a fiber pigtailed external cavity tunable laser, the light of which passed through a fiber polarization controller, an objective (which collimated the beam), two free-space polarizers and a free-space $\lambda/2$ waveplate. The polarization controller generated a linear polarization along the axes

#213127 - $15.00 USD Received 30 May 2014; revised 3 Jul 2014; accepted 7 Jul 2014; published 14 Jul 2014

of the two polarizers, which were parallel to each other. As a result, after the second polarizer, suppression of the cross polarization was better than 60 dB at 1550 nm. The λ/2 waveplate then defined the polarization at the input of the fiber under characterization. An objective was used to couple light into fiber. To ensure that the measured light propagated via the core, another objective was used at the PCF output to obtain an image of its output and an iris was placed on the image plane to block cladding light. The input polarization was then varied by rotating the waveplate and input and output powers were measured for each waveplate angle. The fiber transmittance was calculated as the ratio between the output and the input power for each polarization angle. It is noted that this setup scans only linear polarizations since both the fiber symmetry and simulation results indicate that the tapered fiber's eigenstates are linearly polarized.

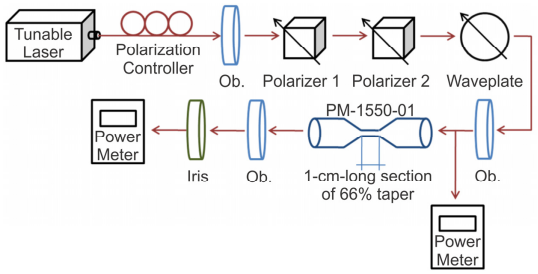

Fig. 4. Optical characterization setup. Ob.: objective lens.

It is noted that the waveplate imposes a limitation on the highest measurable PDL with this setup. As it is designed to operate at 1550 nm (and it has a nominal retardation accuracy of ± λ/300), its exit polarization is slightly elliptical when it is not parallel to one of its principal axes, especially as the wavelength is tuned. To minimize the impact of this feature on the experiment, an initial characterization was made to determine the tapered PCF's axes of highest and lowest transmission. The two polarizers were then rotated so that their axes were parallel to the fiber axis of minimum transmittance (so that, in this case, the waveplate axes were also aligned, minimizing polarization ellipticity). The polarization controller was adjusted accordingly to maximize power through the polarizers. Fiber transmittance was then measured as a function of polarization angle as described above. The PCF's nominal polarization extinction ratio (>30 dB in 100 m), which is related to the residual coupling between orthogonal polarization modes, is assumed to be sufficiently high so that polarization coupling can be neglected along the fiber.

The results of the optical characterization can be seen in Fig. 5. Figure 5(a) shows the transmittance at 1560 nm as a function of input polarization angle. As expected for a polarizing element, it exhibits a sinusoidal behavior. The PDL can then be calculated as the ratio between maximum and minimum transmittance. Figures 5(b) and 5(c) show the variation of the PDL with wavelength for two different fabricated samples. It can be seen that the resulting structures are polarizing across the entire characterized spectral range of 1510-1600 nm, with values not lower than 7 dB and 12 dB in the case of samples 1 and 2, respectively. The highest measured PDL value was 35.3 dB/cm (at 1544 nm, for sample 1). It is noted that, unlike numerically predicted, the PDL spectra do not exhibit a monotonic increase with wavelength, presenting numerous peaks and valleys. It is believed that this is a consequence of resonant coupling between core guided and cladding radiation, increasing the core loss for the lossier polarization. Many of such resonances could take place along the taper transition region (at various positions), which was not accounted for in the simulation. These resonances are likely to be highly dependent on the exact fiber structure, which may explain the differences in the PDL spectra for samples 1 and 2. Indeed, simulations show that even the PDL spectrum obtained from Fig. 2(c), which neglects the taper transition region, varies by up to 3.4 dB/cm and 26.0 dB/cm when d and d' vary by 2%, respectively.

#213127 - $15.00 USD Received 30 May 2014; revised 3 Jul 2014; accepted 7 Jul 2014; published 14 Jul 2014

The transmittance obtained experimentally at 1550 nm was up to 15% at the lower loss polarization. Considering that at least 50% of loss occurs during the coupling of light into the fiber, the insertion loss of the tapered region is estimated to be at maximum of 25% (~1.2 dB). This value is lower than expected by simulation (5.4 dB/cm and ~10 dB/cm with the down-scaled original PCF cross section and with the cross section shown in Fig. 1(b), respectively), possibly due to the previously mentioned fiber's sensitivity to variations on the actual structure.

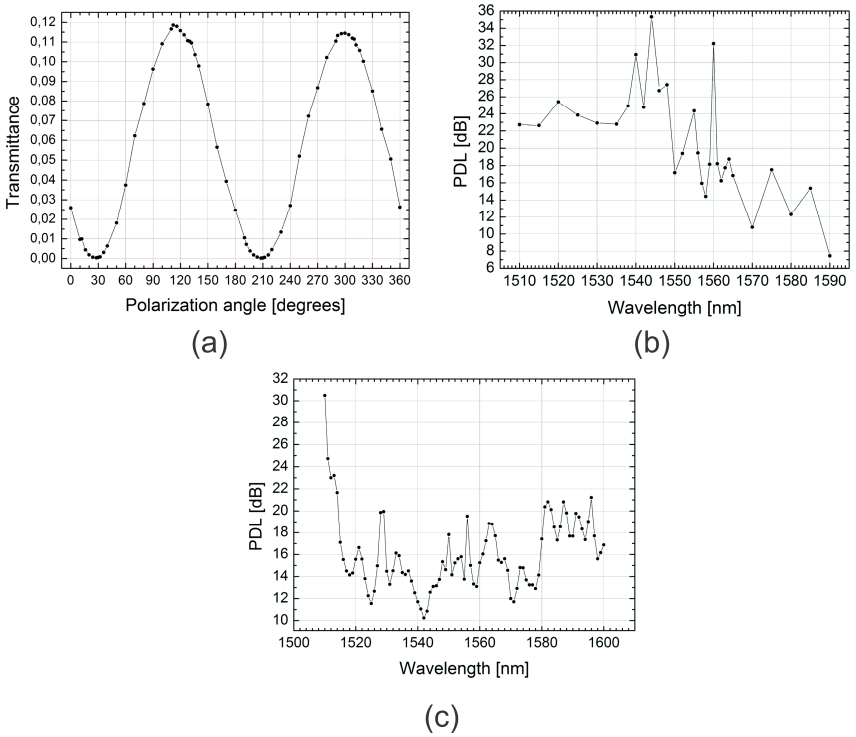

Fig. 5. (a) Fiber transmittance as a function of input polarization angle at 1560 nm. Measured PDL spectra in the 1510-1600 nm range for tapered PCF samples 1 (b) and 2 (c).

5. Conclusions

We proposed and demonstrated a high PDL fiber section through downscaling of a commercial highly birefringent PCF, which is achieved by tapering with differential pressure applied to the holes. The taper waist, with a 66% scale reduction, was 1 cm long and was polarizing in the 1510-1600 nm wavelength range. A maximum polarization dependent loss of 35.3 dB/cm was measured, which is considerably higher than those of commercial (non PCF) polarizing fibers and then most of those experimentally demonstrated with polarizing PCFs. Furthermore, the resulting structure and production of the high PDL section are demonstrated to be extremely simple. Also, the short high PDL section is obtained in an otherwise polarization maintaining PCF, allowing for the creation of an integrated system in which the high PDL section is made directly on the polarization maintaining fiber. This makes these two regions be perfectly aligned to each other, and avoid splice losses and unwanted reflections in splices.

Acknowledgments

The authors thank CAPES, Mackpesquisa, INCT Fotonicom (CNPq and FAPESP) and FINEP (SIA Project- proc. 0.1.06.1177.00) for financial support.